PCCP

Accepted Manuscript

ROYAL SOCIETY OF CHEMISTRY

www.rsc.org/pccp

Pressure induced speciation changes in the aqueous Al^{3+} system.

Stuart Bogatko, Paul Geerlings

Eenheid Algemene Chemie, Vrije Universiteit Brussel (VUB), Faculteit Wetenschappen,
Pleinlaan 2,
1050 Brussels, Belgium.

CORRESPONDING AUTHOR FOOTNOTE:

Email: stuart.bogatko@gmail.com

Telephone: +32-2-629-3316

Abstract

We have developed a simple model for incorporating the influence of external pressure and solution pH into a cluster based (i.e. comprising the central Al^{3+} cation and nearest neighbor coordinating H_2O and OH^- ligands) 1st principles approach to investigate the hydrolysis equilibria of aqueous Al^{3+} monomeric species in high pressure environments such as are found in the Earth's mantle. Our model is demonstrated to reproduce the well documented bulk chemistry of the aqueous Al^{3+} system under ambient conditions, namely the system is dominated at low and high pH by the 6-coordinated aqua species and 4 coordinated hydroxide species, respectively, while all remaining species occupy a narrow intermediate pH range. Coupling this model to changes in solution pH is achieved by using $[H_3O^+]$ as a parameter in the definition of the formation equilibrium constants used; the influence of external pressure is evaluated using Planck's equation. This approach predicts that changes in external pressure will induce drastic changes in the aqueous solubility of these species under high pressure conditions and moderate changes as low as 5GPa. Finally, some industrial and geochemical implications of this result are discussed.

Keywords: Aqueous Al^{3+}, speciation, high pressure, solubility.

Introduction

The speciation of the aluminum(III) ion is of broad interest to many areas, notably in the geochemical, industrial and environmental sectors of the chemical sciences. The geochemical interest arises from the high natural abundance of aluminum and thus its non-negligible influence on the Earth's chemistry. The industrial interest is illustrated by the well-known Bayer-process by which bauxite is refined to form pure alumina; Al^{3+} species are also liberated in the process to recover hydrocarbons from deep deposits.[1] The environmental interest arises from the toxic properties of many Al^{3+} species, which disrupt essential biological processes in plants and animals and may possibly play a role in Alzheimer's disease.[2,3] Contact with the aqueous phase would undoubtedly play a major role in the migration of aluminum species. In solution Al^{3+} exists in a variety of oxohydroxo polyion species such as $Al(H_2O)_6^{3+}$, $Al_2(OH)_2(H_2O)_8^{4+}$, $Al_3(OH)_4(H_2O)_9^{5+}$, $Al_4(OH)_6(H_2O)_{11}^{6+}$, $Al_4O(OH)_5(H_2O)_{10}^{5+}$ and $AlO_4Al_{12}(OH)_{24}(H_2O)_{12}^{7+}$ as well as with other ligands.[3–8] The complexity of this aqueous system has made it difficult to develop a successful speciation model due to uncertainties in the exact nature and structure of even the smallest polymer species.[9–14] This uncertainty only increases when considering aluminum speciation under extreme conditions such as high pressure. For example, there remains disagreement on the basic transport properties of mantle aluminum: some results suggesting the presence of mobile aqueous species while others suggest otherwise.[15–20] Resolving this issue would lead to an improved model of aqueous Al^{3+} chemistry. This would lead to an increased understanding of the speciation of aqueous Al^{3+} under high pressure conditions, allowing for better prediction of mantle processes to be made. Another potential benefit would be the more accurate prediction of the solubility of aqueous aluminum species. This, in turn, would have direct consequences for the future of cleaner industrial processes and more efficient environmental remediation strategies.

Not surprisingly, aluminum speciation is the focus of many experimental studies using, for example, neutron and X-Ray diffraction, NMR, and Mass Spectrometry techniques.[21–23] However, the complexity of the Al speciation pattern mentioned above also creates significant problems for experimental characterization of these species. This is especially true near neutral pH conditions where a large variety of Al^{3+} species form and where, arguably, the most interesting chemistry is occurring such as polymerization and precipitation. Researchers often turn to theoretical methods, namely molecular modeling, either as a supplement to their experimental observations or as a predictive tool in itself in studies of aqueous Al^{3+}.[11,24–27] However, the problem of system complexity remains in these approaches and work is often limited to a sharp focus on one or a few molecular species, in spite of the vast complexity of the system.

We have been very active in theoretical studies of aqueous Al^{3+} focusing on the fundamental mechanisms of speciation[28–32]. A unique aspect of our approach is that we have decomposed the aqueous aluminum system into fundamental reactions corresponding to hydrolysis and dehydration of the Al^{3+} species. Estimating the equilibrium constants of these reactions from first principles gives us the capability to compute mole fraction values for each individual species included in our model as a function of solution pH. This allows us to make qualitative predictions about changes in bulk solution composition in response to changes in environmental conditions. Our results have focused on elucidating the high degree of complexity in the monomeric Al^{3+} hydrolysis products arising from a mechanism dubbed cooperativity among the Al^{3+} hydrolytic species.[33] To this end, polymerization of Al^{3+} species and interaction with geochemically relevant species[18,20,34,35] have been neglected. In our previous work, our efforts had been restricted to investigations under ambient pressure conditions. Here we demonstrate how to extend our model to include the effect of external pressure and discuss how our results shed light on natural processes, namely aqueous Al^{3+} speciation, occurring in high pressure environments, such as the Earth's mantle where pressures up to ~135 GPa exist[36], and may help direct the formulation of cleaner industrial processing of aluminum ore. Finally, in our aim to describe pressure induced speciation of aqueous Al^{3+} we make no attempt to describe the influence of temperature on these equilibria. While temperature is certainly a relevant variable, it and associated phenomena such as ion pairing, which indeed play a role in such a system,[35] and phase transitions are neglected. Rather, our aim is to firmly establish and describe the qualitative link between monomeric Al^{3+} speciation and external pressure via the cooperativity mechanism among monomeric Al^{3+} hydrolysis species.

Methods

The aqueous Al^{3+} system is approximated by the set of equilibrium reactions described by equation 1,

$$Al(H_2O)_6^{3+} + xH_2O \rightleftharpoons Al(OH)_x(H_2O)_y^{(3-x)+} + xH_3O^+ + (6-x-y)H_2O, \qquad 1$$

where x ranges from 0 to 4 and $x+y$ ranges from 4 to 6. The corresponding change in molar volume of equation 1 is found by evaluating equation 2,

$$\Delta V = \left(V^{x,y} + xV^{H_3O^+} + (6-x-y)V^{H_2O}\right) - (V^{0,6} + xV^{H_2O}), \qquad 2$$

where $V^{x,y}$, $V^{H_3O^+}$ and V^{H_2O} refer to the molar volumes of the $Al(OH)_x(H_2O)_y^{(3-x)+}$ species (via equation 3 below), hydronium ion and water molecule.

The simplest expression for the volume of a monomeric aqueous metal cation is $V = \frac{4}{3}\pi r^3$ where r is the radial distance from a metal center enclosing a region of solvent which is perturbed relative to a bulk water structure. For most if not all aqueous metal species, the perturbation in bulk solvent structure does not extend in any significant way beyond the formation of one or two radially structured solvation shells (a.k.a 1st and 2nd hydration shells). The estimation of the volume of an aqueous metal species is here achieved using the average metal-oxygen distance of the 1st shell coordinating waters with 1.4Å added corresponding to half the oxygen-oxygen distance of a moderately strong H-bond[37] as in equation 3.

$$V = \frac{4}{3}\pi(\langle M - OH_2\rangle + 1.4)^3 \qquad 3$$

This corrected distance thus corresponds to the midpoint between the 1st and 2nd hydration shells of an aqueous metal species. A study of the effects of variation of this distance on our results that supports this simple definition is provided in the supporting information. Note here that this is a somewhat heavy handed approximation as the 1st and 2nd hydration shell structure may change significantly for hydrolysis species (see Bogatko[38] and references therein). These volumes are per particle, Molar volumes are computed by multiplying by N_A (6.022×10^{23}

particles per mole). Other approaches to estimating the molar volume of an aqueous species exist.[39,40] We follow this method because it is straightforwardly implemented to our previous data set.[31] To keep the molar volumes for the H_2O and H_3O^+ molecules on equal footing we opted to use molar volumes founded on similar grounds, namely by constructing a radius based on average O-H distances and an offset of 1.6Å. The increased offset, relative to 1.4Å used in equation 3 is included to account for a slightly weaker H-bonding interaction for the H_2O and H_3O^+ molecules with a bulk water environment. While more accurate approaches exist to estimate these distances,[41] we have elected to remain at this qualitative level.

The inclusion of pressure is achieved by using a method based on Planck's equation[42] (equation 4), which may be considered as a pressure analog of the van‘t Hoff equation for temperature,

$$RT\left(\frac{\partial lnK}{\partial P}\right)_T = -\Delta V, \qquad 4$$

in which the logarithm of the equilibrium constant, K, is sensitive to pressure, P, in proportion to changes in molar volume (ΔV) of the reactants and products.[43–45] Our work is based on a finite difference approach under which Planck's equation becomes equation 5,

$$RT\left(\frac{lnK_1 - lnK_0}{P_1 - P_0}\right)_T = -(V_P - V_R) = -\Delta V, \qquad 5$$

where V_P and V_R are the total molar volumes of product and reactant species as in equation 2. We note here that this implies the approximation that all species are incompressible.[43–45] Rearranging equation 5 yields an equation to evaluate the equilibrium constant K_1 at pressure P_1 based on known K_0, P_0 and constant temperature, T.

$$K_1 = K_0 e^{\left(\frac{-\Delta V}{RT}\right)\times(P_1 - P_0)} \qquad 6$$

Estimates of equilibrium constants were achieved on a quantum chemical basis by revisiting the species investigated in our previous study wherein the aqueous aluminum systems was investigated under ambient conditions from 1st principles, namely the $Al(OH)_x(H_2O)_y^{(3-x)+}$ complexes.[31] Namely, 14 aqueous Al^{3+} species, sampling water and hydroxide coordination, were investigated using density functional theory (DFT)[46–48] calculations with the B3LYP[49,50] exchange correlation functional and the 6-311++G(d,p) basis set[51] using the Gaussian ’03 package.[52] This level of theory has been demonstrated to provide a good representation of the Al^{3+} water interaction.[26,28,53,54] The geometry of each species was optimized in gas phase followed by a normal mode analysis to ensure that they corresponded to a true minimum, e.g. no negative frequencies were detected. The Gibbs Free energies with solvation free energy correction were then computed and used to compute the K_0 corresponding to equation 1 using $K_0 = e^{-\Delta G/RT}$. The effect of the water solvent was included by embedding these species in a continuum solvent modeled using the IEF-PCM formalism[55,56] with a water dielectric constant of 78.39, ionic strength of 0 and the United Atom Topological Model (UAKS) parameter set. This included a correction to the standard state Gibbs Free Energy of RTln(24.46) for changing from a standard state of 1 atm to 1 mol/L.[57–59] It is well known that this approximation may affect calculated properties such as hydrolysis equilibria. We have previously reported that an explicit 2nd hydration shell induces a significant reduction in the hydrolysis free energy of an aqueous

Al^{3+} monomer species.[31] The inclusion of explicit solvating waters has been extensively studied by Wander et al.[26], Dixon et al.[60] and Kubicki[61] and has been shown to, for example, bring calculated pKa values for aqueous Al^{3+} to closer agreement with experiment.[26] An explicit, extended hydration region also comes at significant computational expense, however, and as we have argued in our previous studies, the qualitative chemical picture that we are aiming to describe remains intact with the present level of theory.

Because our reaction equilibrium constants (K_0) were computed for geometries optimized in gas phase, the corresponding external pressure is set to zero (P_0=0) in equation 6 to yield

$$K_1 = K_0 e^{\left(\frac{-\Delta V \times P_1}{RT}\right)}. \qquad 7$$

The use of 0 GPa is somewhat different from the environment modeled in the IEF-PCM calculation, which is implicitly 1 atm (~1.0x10^{-4} GPa). However, the pressures we are interested in (up to ~100GPa) suggest to us that this discrepancy is of extremely minor importance. Specifically, P_0 equal to 0 or 1.0x10^{-4} GPa yields 1 or 1.002 for the value of the $e^{\left(\frac{-\Delta V \times P_0}{RT}\right)}$ term in equation 7 using a ΔV of 10ml. Mole fractions of the aqueous Al^{3+} species are computed using equation 8 below

$$\left[Al(OH)_x(H_2O)_y^{(3-x)+}\right] = K^{x,y} \times [Al(H_2O)_6^{3+}] \times [H_3O^+]^{-x} \times [H_2O]^{-(6-2x-y)} \qquad 8$$

Where the $K^{x,y}$ are the corresponding equilibrium constants for the reaction described in equation 1 resulting in the formation of the $Al(OH)_x(H_2O)_y^{(3-x)+}$ species from $Al(H_2O)_6^{3+}$. The total concentration of Al^{3+} in the model system is given by equation 9.

$$[Al^{3+}] = \sum_{x,y} K^{x,y} \times [Al(H_2O)_6^{3+}] \times [H_3O^+]^{-x} \times [H_2O]^{-(6-2x-y)} \qquad 9$$

For simplicity we have chosen $[Al^{3+}] = 1$ and thus compute mole fractions. We also assume $[H_2O]$=55.5 (Molarity of water at 298.15K) and use $[H_3O^+]=10^{-pH}$ (M) as a free parameter. Using this result we may express the equilibrium concentrations of each Al^{3+} hydrolyisis products under varying pH and external pressure conditions.

Results and Discussion

The average M-O distance itself and with 1.4Å offset, molar volume values and equilibrium constants, K_0, computed for each $Al(OH)_x(H_2O)_y^{(3-x)+}$ species are supplied in table I. The ΔV associated with the reactions described by equation 1, when evaluated with these and the molar volumes of H_2O and H_3O^+ (10.103 and 10.342 ml, respectively using average O-H distances of 0.96Å and 0.98Å), are provided graphically in Figure 1 for each species. We reiterate here that to keep our molar volume estimates for the H_2O and H_3O^+ molecules on equal footing to those of the $Al(OH)_x(H_2O)_y^{(3-x)+}$ species, we opted to use molar volumes calculated by constructing a radius based on average O-H distances and an offset of 1.6Å to account for the H-bonding interaction for the H_2O and H_3O^+ molecules with a bulk water environment. Also provided in Figure 1 are the individual contributions from inserting water molecules into the bulk solvent (i.e. our molar volume estimate for water, 10.103ml, multiplied by the number of waters inserted into the bulk), geometrical changes in the Al species (change in molar volume relative to $Al(H_2O)_6^{3+}$) and a contribution from inserting a proton into the bulk solvent estimated as the difference in molar volumes of H_2O and H_3O^+ species. The net ΔV of these reactions are clearly dominated by the term corresponding to the insertion of a water molecule into the bulk solvent, which is much larger than those corresponding to the molecular rearrangement of the Al^{3+} complexes and the proton to solvent transfer. That the net ΔV is in all cases dominated by the insertion of a water molecule into the bulk solvent appears to justify our approach, which is aimed at recovering a qualitative relationship between external pressure and Al^{3+} hydrolysis behavior. As we discussed in our earlier work, these aqueous Al^{3+} species exhibit a property known as *cooperativity* among their hydrolysis products. A main consequence of *cooperativity* is that the hydrolysis facilitates a reduction in water coordination which in turn facilitates further hydrolysis. That the ΔV of these reactions are uniformly dominated by the water ligand to bulk transfer, along with the coupling of water ligand loss to increased hydrolytic strength, suggests to us that these reactions should be, via Planck's equation, sensitive to external pressure.

We examine this conjecture in Figure 2 where we have computed the mole fraction of each of the $Al(OH)_x(H_2O)_y^{(3-x)+}$ species as a function of solution pH at pressures ranging from 0 to 50 GPa. In Figure 2A, the species distribution at 0GPa reflects what we and others have predicted[31] and observed[33] for aqueous Al^{3+} speciation. Namely that the 6 coordinated aqua $Al(H_2O)_6^{3+}$ species dominates at low pH, the 4 coordinated $Al(OH)_4^{1-}$ species dominates at high pH while at intermediate pH the remaining $Al(OH)_x(H_2O)_y^{(3-x)+}$ are crowded in a narrow pH region. The crowding of these species is a result of the aforementioned cooperativity mechanism. The main result accompanying an increase in the external pressure to 1GPa is described in Figure 2B as a roughly uniform shift of the entire species distribution to higher pH by roughly 1 pH unit. However, the species distribution under an external pressure of 10GPa (Figure 2C) clearly shows a very dramatic change in hydrolysis behavior wherein species with coordination numbers less than 6 have been partially suppressed. This suppression is complete at higher external pressures as indicated in Figure 2D, showing only 6 coordinated species under external pressures of 50GPa.

The predicted influence of external pressure on Al^{3+} coordination is illustrated in Figure 3 wherein the average total coordination number of all species is plotted against solution pH for 8 contours corresponding to external pressures of 0, 0.1, 1, 5, 10, 20, 50 and 100 GPa. The data presented in this figure more clearly indicates that the composition of the aqueous Al^{3+} system is perturbed by external pressure in such a way that the 6 coordinate species become more favorable. The explanation for this perturbation arises from the influence external pressure exerts on changes in coordination number of the Al^{3+} aqueous complexes. Namely, an increasing external pressure introduces an increasingly greater free energy penalty to the reaction wherein a water ligand is transferred from the Al^{3+} complex to the bulk resulting in a shift in the equilibrium constant favoring the formation of the water coordinated species.

To understand how this may affect the hydrolytic properties of the aqueous Al^{3+} species, we analyze their pressure induced changes more carefully in Figures 4A through 4E. These figures show the evolution of the mole fraction distributions of the aqua species (x=0 in the formula $Al(OH)_x(H_2O)_y^{(3-x)+}$; Figure 4A) and the 1st (x=1; Figure 4B), 2nd (x=2; Figure 4C), 3rd (x=3;

Figure 4D) and 4th (x=4; Figure 4E) hydrolysis products at 0, 0.1, 1, 5, 10, 20, 50 and 100 GPa. A central observation from Figure 4 is that the species distributions extend into higher pH regimes as external pressure increases. This alteration is quite different for each hydrolysis product but can be rationalized as follows. At 0GPa, the model aqueous Al^{3+} system is dominated at low pH by the aqua species and at high pH by the 4th hydrolysis product; the remaining 1st, 2nd and 3rd hydrolysis products have distributions with peaks clustered near ~5pH units. As can be seen in Figure 3, this region coincides with the transition from average coordination number of 6 to 4. The transition from a 6 to a 4 coordination coinciding with clustering of hydrolytic species in a small pH range is in complete agreement with the aqueous Al^{3+} system being governed by the cooperativity mechanism. As pressure increases, however, the changes in species distributions suggest that the influence of this mechanism has lifted. This is indicated by noting that the peaks of the 1st, 2nd and 3rd hydrolysis species are no longer clustered and are separated by many pH units at higher pressures. Furthermore, comparing, for example, the 10GPa contours of Figures 3 and 4 indicate that the aqua and 1st, 2nd and 4th hydrolysis products are 6 coordinated. The system remains 6 coordinated until a pH of roughly 10 after which the 4 coordinate $Al(OH)_4^{1-}$ species dominates.

We should here point out that the transition to a 4 coordinate $Al(OH)_4^{1-}$ species is an implicit part of our model because higher coordination states of the form $Al(OH)_4(H_2O)_y^{1-}$ are not included. We, therefore, cannot reliably say whether or not such species will play a role in aqueous Al^{3+} speciation under high pressure. On the other hand, we also cannot see how such coordination states will drastically change the qualitative picture we have observed on the lower hydrolysis products and thus are confident with this approach.

The pressure induced changes observed in mole fraction distributions of the 3rd hydrolysis product are particularly interesting. These neutral aqueous species precipitate to form aluminum hydroxide solid phases.[62,63] As shown in Figure 4D, the mole fraction of $Al(OH)_3^{0+}$ species is peaked near pH 5. The magnitude of the peak (~1x10^{-4}) indicates a small relative amount of these species are predicted. This peak gradually shifts to higher pH as external pressure increases. The interpretation of this is that the pH conditions under which insoluble $Al(OH)_3^{0+}$ readily forms undergo significant changes as external pressure increases. Large changes in the aqueous stability of $Al(OH)_3^{0+}$ may be interpreted as indicating large changes in the solubility of solid aluminum hydroxide phases under high pressure. More plainly put, these results indicate the possibility of an aluminum hydroxide solid phase that precipitates near neutral pH conditions under ambient pressure conditions may dissolve under high pressure conditions.

This general notion appears to support claims by some that Al^{3+} is mobile in the earth's mantle,[15–18,20] where pressures may reach many GPa. Our model suggests that changes in aqueous Al^{3+} speciation under these pressures is in the direction of increased aqueous solubility of Al^{3+} species. High pressure induced solubility changes of Al^{3+} species may also be of great industrial use. For example, the refinement of aluminum involves the dissolution of a solid aluminum hydroxide phase, Bauxite.[1] Currently this is achieved by the Bayer-Process, a process that involves the use of highly corrosive chemicals with an end result of essentially untreatable waste.[1] If the high pressure solubility of Al^{3+} species is found to be achievable in Industrial class reactors, this result may lead to a cleaner Bauxite processing method.

Conclusions

We present a simple model for incorporating the influence of external pressure on cluster based (i.e. comprising the central Al^{3+} cation and nearest neighbor coordinating H_2O and OH^- ligands) 1st principles investigations of the hydrolysis equilibria of aqueous Al^{3+} monomeric species. The confidence in our model rests on its ability to reproduce the qualitative bulk chemistry of the aqueous Al^{3+} system under ambient conditions, namely the system is dominated at low and high pH by the 6-coordinated aqua species and 4 coordinated hydroxide species, respectively, while all remaining species occupy a narrow intermediate pH range. Coupling this model to changes in external pressure is achieved by incorporating the pressure dependence of the equilibrium constant based on Planck's equation. This approach predicts that changes in external pressure will significantly perturb the speciation of aqueous Al^{3+}. A main consequence is observed by noting large changes in neutral $Al(OH)_3$ species, which indicate drastic changes in the aqueous solubility of these species are occurring under high pressure conditions and moderate changes as low as 5GPa of external pressure. The mechanism by which this is achieved arises from the observed cooperativity mechanism operating in aqueous Al^{3+} hydrolysis products, a critical step being the liberation of a coordinating water molecule to facilitate further hydrolysis of the remaining waters. Increased external pressures hinder this process, greatly altering the aqueous Al^{3+} hydrolytic properties. This result is in line with some indications that aqueous Al^{3+} is mobile in the earth's mantle, where extreme pressure environments exist, and points to possible cleaner industrial processing of aluminum ore such as Bauxite.

Due to some approximations adopted in its development, this should be considered a qualitative model. We consider that the necessary elements to include in order achieve a quantitative description are the effects of an extended solvation region (beyond a 1st hydration shell), the formation of aluminum polymer species and interactions with other relevant species.

Acknowledgements

This work has been conducted within the context of a VUB strategic research program for which S.B. has been active as a postdoctoral associate. P.G. also thanks the VUB and FWO for continuous support of his research group.

References

1. T. W. Swaddle, *Coord. Chem. Rev.*, 2001, **219-221**, 665–686.
2. R. A. Yokel, *J. Alzheimers Dis.*, 2006, **10**, 223–253.
3. J. I. Mujika, E. Rezabal, J. M. Mercero, F. Ruipérez, D. Costa, J. M. Ugalde, and X. Lopez, *Comput. Struct. Biotechnol. J.*, 2014, **9**.
4. W. H. Casey, *Chem Rev*, 2005, **106**, 1–16.
5. A. Singhal and K. D. Keefer, *J. Mater. Res.*, 1994, **9**, 1973–1983.
6. S. Pál, *J. Mol. Liq.*, 2009, **146**, 1–14.
7. J. W. Akitt and A. Farthing, *J Chem Soc Dalton Trans*, 1981, 1624–1628.
8. A. L. O. de Noronha, L. Guimarães, and H. A. Duarte, *J. Chem. Theory Comput.*, 2007, **3**, 930–937.
9. A. C. Fournier, K. L. Shafran, and C. C. Perry, *Anal. Chim. Acta*, 2008, **607**, 61–73.
10. A. Sarpola, H. Hellman, V. Hietapelto, J. Jalonen, J. Jokela, J. Rämö, and J. Saukkoriipi, *Polyhedron*, 2007, **26**, 2851–2858.
11. A. Sarpola, V. Hietapelto, J. Jalonen, J. Jokela, and R. S. Laitinen, *J. Mass Spectrom.*, 2004, **39**, 423–430.
12. A. Sarpola, V. Hietapelto, J. Jalonen, J. Jokela, R. S. Laitinen, and J. Rämö, *J. Mass Spectrom.*, 2004, **39**, 1209–1218.
13. C. C. Perry and K. L. Shafran, *J. Inorg. Biochem.*, 2001, **87**, 115–124.
14. K. L. Shafran and C. C. Perry, *Dalton Trans*, 2005, 2098–2105.
15. G. M. Anderson and C. W. Burnham, *Am. J. Sci.*, 1983, **283-A**, 283–297.
16. T. Beitter, T. Wagner, and G. Markl, *Contrib. Mineral. Petrol.*, 2008, **156**, 689–707.
17. C. E. Bucholz and J. J. Ague, *J. Metamorph. Geol.*, 2010, **28**, 19–39.
18. C. E. Manning, *J. Geochem. Explor.*, 2006, **89**, 251–253.
19. B. W. D. Yardley, *J. Geol. Soc.*, 2009, **166**, 585–600.
20. P. Tropper and C. E. Manning, *Chem. Geol.*, 2007, **240**, 54–60.
21. A. M. Gaspar, M. A. Marques, M. I. Cabaço, M. I. de B. Marques, A. I. Kolesnikov, J. Tomkinson, and J.-C. Li, *J. Phys. Condens. Matter*, 2004, **16**, 6343.
22. W. Bol and T. Welzen, *Chem. Phys. Lett.*, 1977, **49**, 189–192.
23. A. T. Sarpola, J. J. Saukkoriipi, V. K. Hietapelto, J. E. Jalonen, J. T. Jokela, P. H. Joensuu, K. E. Laasonen, and J. H. Rämö, *Phys Chem Chem Phys*, 2007, **9**, 377–388.
24. T. W. Swaddle, J. Rosenqvist, P. Yu, E. Bylaska, B. L. Phillips, and W. H. Casey, *Science*, 2005, **308**, 1450–1453.
25. J. Wang, J. R. Rustad, and W. H. Casey, *Inorg. Chem.*, 2007, **46**, 2962–2964.
26. M. C. F. Wander, J. R. Rustad, and W. H. Casey, *J. Phys. Chem. A*, 2010, **114**, 1917–1925.
27. R. J. Evans, J. R. Rustad, and W. H. Casey, *J. Phys. Chem. A*, 2008, **112**, 4125–4140.
28. S. Bogatko, E. Cauët, and P. Geerlings, *J. Am. Soc. Mass Spectrom.*, 2013, **24**, 926–31.
29. S. Bogatko, E. Cauët, and P. Geerlings, *J Phys Chem C*, 2011, **115**, 6910–6921.
30. S. Bogatko and P. Geerlings, *Phys. Chem. Chem. Phys.*, 2012, **14**, 8058–8066.
31. S. Bogatko, J. Moens, and P. Geerlings, *J Phys Chem A*, 2010, **114**, 7791–7799.
32. S. Bogatko, E. Cauët, and P. Geerlings, *Phys. Chem. Chem. Phys.*, 2013, **15**, 15309–15311.
33. B. Martin, *J. Inorg. Biochem.*, 1991, **44**, 141–147.
34. C. E. Manning, *Earth Planet. Sci. Lett.*, 2004, **223**, 1–16.
35. S. Schrödle, W. W. Rudolph, G. Hefter, and R. Buchner, *Geochim. Cosmochim. Acta*, 2007, **71**, 5287–5300.
36. A. M. Dziewonski and D. L. Anderson, *Phys. Earth Planet. Inter.*, 1981, **25**, 297–356.
37. I. D. Brown, *Acta Crystallogr. Sect. A*, 1976, **32**, 24–31.
38. S. A. Bogatko, Ph.D., Chemistry, University of California, San Diego, 2008.
39. D. Spångberg, M. Wojcik, and K. Hermansson, *Chem. Phys. Lett.*, 1997, **276**, 114–121.

40. K. Hermansson and M. Wojcik, *J. Phys. Chem. B*, 1998, **102**, 6089–6097.
41. C.-G. Zhan and D. A. Dixon, *J. Phys. Chem. A*, 2001, **105**, 11534–11540.
42. M. Planck, *Ann. Phys.*, 1887, **32**, 462.
43. N. A. North, *J Phys Chem*, 1973, **77**, 931–934.
44. D. A. Lown, H. R. Thirsk, and Lord Wynne-Jones, *Trans Faraday Soc*, 1968, **64**, 2073–2080.
45. B. B. Owen and S. R. Brinkley, *Chem Rev*, 1941, **29**, 461–474.
46. W. Kohn and L. J. Sham, *Phys. Rev.*, 1965, **140**, A1133–A1138.
47. W. Kohn and L. J. Sham, *Phys. Rev.*, 1965, **137**, A1697–A1705.
48. L. J. Sham and W. Kohn, *Phys. Rev.*, 1966, **145**, 561–567.
49. A. D. Becke, *J. Chem. Phys.*, 1993, **98**, 5648–5652.
50. C. Lee, W. Yang, and R. G. Parr, *Phys. Rev. B*, 1988, **37**, 785–789.
51. W. J. Hehre, L. Radom, P. von R. Schleyer, and J. Pople, *AB INITIO Molecular Orbital Theory*, Wiley-Interscience, 1st edn., 1986.
52. M. J. Frisch, G. W. Trucks, H. B. Schlegel, G. E. Scuseria, and M. A. Robb, J. R. Cheeseman, G. Scalmani, V. Barone, B. Mennucci, G. A. Petersson, H. Nakatsuji, M. Caricato, X. Li, H. P. Hratchian, A. F. Izmaylov, J. Bloino, G. Zheng, J. L. Sonnenberg, M. Hada, M. Ehara, K. Toyota, R. Fukuda, J. Hasegawa, M. Ishida, T. Nakajima, Y. Honda, O. Kitao, H. Nakai, T. Vreven, J. A. Montgomery, Jr., J. E. Peralta, F. Ogliaro, M. Bearpark, J. J. Heyd, E. Brothers, K. N. Kudin, V. N. Staroverov, T. Keith, R. Kobayashi, J. Normand, K. Raghavachari, A. Rendell, J. C. Burant, S. S. Iyengar, J. Tomasi, M. Cossi, N. Rega, J. M. Millam, M. Klene, J. E. Knox, J. B. Cross, V. Bakken, C. Adamo, J. Jaramillo, R. Gomperts, R. E. Stratmann, O. Yazyev, A. J. Austin, R. Cammi, C. Pomelli, J. W. Ochterski, R. L. Martin, K. Morokuma, V. G. Zakrzewski, G. A. Voth, P. Salvador, J. J. Dannenberg, S. Dapprich, A. D. Daniels, O. Farkas, J. B. Foresman, J. V. Ortiz, J. Cioslowski, and D. J. Fox, *Gaussian 09, Revision B.01*, Gaussian, Inc.,, Wallingford CT, 2009., 2010.
53. W. Yang, Z. Qian, Q. Miao, Y. Wang, and S. Bi, *Phys. Chem. Chem. Phys.*, 2009, **11**, 2396–2401.
54. J. Saukkoriipi and K. Laasonen, *J. Chem. Theory Comput.*, 2010, **6**, 993–1007.
55. E. Cancès, B. Mennucci, and J. Tomasi, *J. Chem. Phys.*, 1997, **107**, 3032–3041.
56. J. Tomasi, B. Mennucci, and E. Cancès, *J. Mol. Struct. THEOCHEM*, 1999, **464**, 211–226.
57. C. P. Kelly, C. J. Cramer, and D. G. Truhlar, *J. Phys. Chem. A*, 2006, **110**, 2493–2499.
58. M. D. Liptak and G. C. Shields, *Int. J. Quantum Chem.*, 2001, **85**, 727–741.
59. V. S. Bryantsev, M. S. Diallo, and W. A. Goddard III, *J. Phys. Chem. B*, 2008, **112**, 9709–9719.
60. D. A. Dixon, V. E. Jackson, J. Corbett, and J. R. Rustad, *Geochim. Cosmochim. Acta*, 2010, **74**, A237.
61. J. D. Kubicki, *J. Phys. Chem. A*, 2001, **105**, 8756–8762.
62. D. T. Richens, *The Chemistry of Aqua Ions*, Wiley-Blackwell, 1997.
63. W. H. Casey, J. R. Rustad, and L. Spiccia, *Chem. - Eur. J.*, 2009, **15**, 4496–4515.

Tables

Table I : Average M-O distance itself and with 1.4Å offset, molar volume values and equilibrium constants, K_0, computed for each $Al(OH)_x(H_2O)_y^{(3-x)+}$ species.

Species	$\langle M - OH_2 \rangle$ Å	$\langle M - OH_2 \rangle + 1.4$ Å	V ml	K_0
$Al(H_2O)_6^{3+}$	1.940	3.340	94.01	1.00E+00
$Al(OH)_1(H_2O)_5^{2+}$	1.934	3.334	93.51	1.04E-18
cis-$Al(OH)_2(H_2O)_4^{1+}$	1.944	3.344	94.32	9.12E-24
trans-$Al(OH)_2(H_2O)_4^{1+}$	1.935	3.335	93.58	9.49E-20
$Al(OH)_3(H_2O)_3^{0+}$	1.956	3.356	95.35	3.83E-36
$Al(H_2O)_5^{3+}$	1.898	3.298	90.48	7.54E-12
$Al(OH)_1(H_2O)_4^{2+}$	1.880	3.280	89.04	7.86E-24
$Al(OH)_2(H_2O)_3^{1+}$	1.883	3.283	89.22	3.23E-19
$Al(OH)_3(H_2O)_2^{0+}$	1.896	3.296	90.33	4.87E-25
$Al(H_2O)_4^{3+}$	1.836	3.236	85.50	1.53E-25
$Al(OH)(H_2O)_3^{2+}$	1.808	3.208	83.27	3.29E-33
$Al(OH)_2(H_2O)_2^{1+}$	1.796	3.196	82.33	3.45E-21
$Al(OH)_3(H_2O)_1^{0+}$	1.799	3.199	82.55	1.51E-21
$Al(OH)_4^{1-}$	1.792	3.192	82.01	5.20E-25

Figures

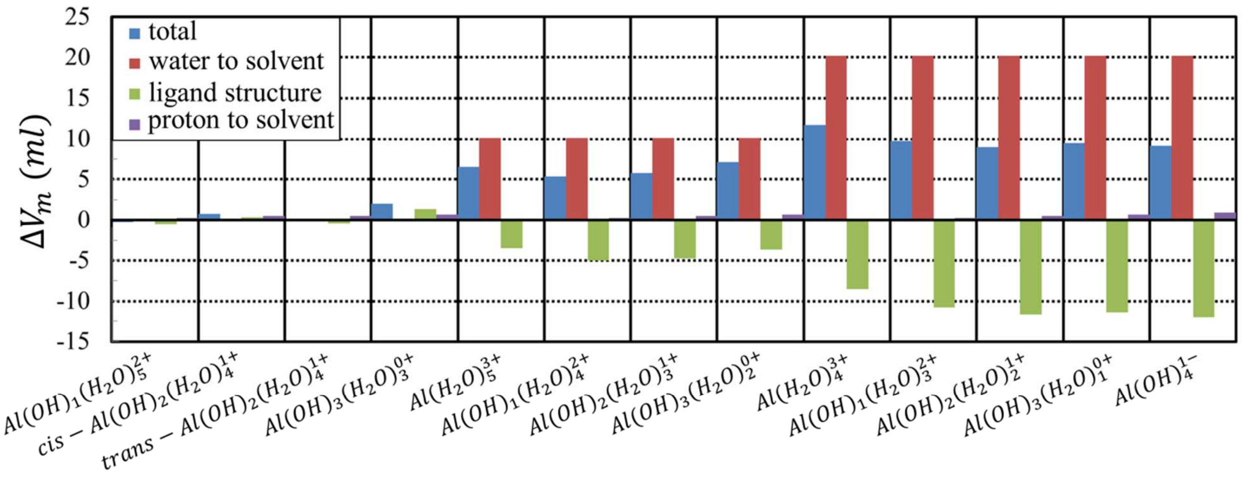

Figure 1: Total delta V, delta V of Al species and delta V from inserting water to bulk.

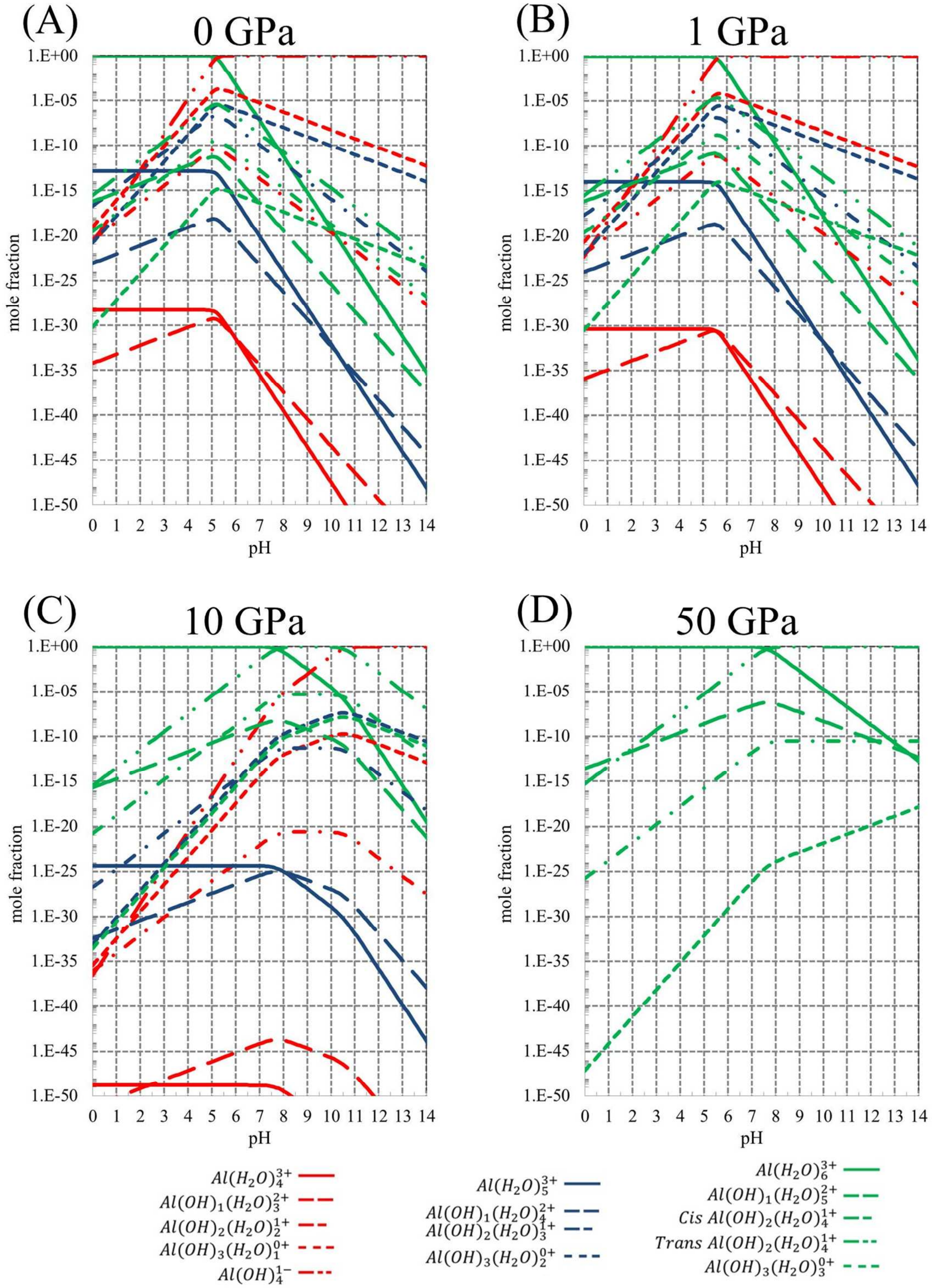

Figure 2: Mole fraction distributions computed at modelled external pressures of 0 (A), 1 (B), 10 (C) and 50 (D) GPa following the procedure outlined in the text.

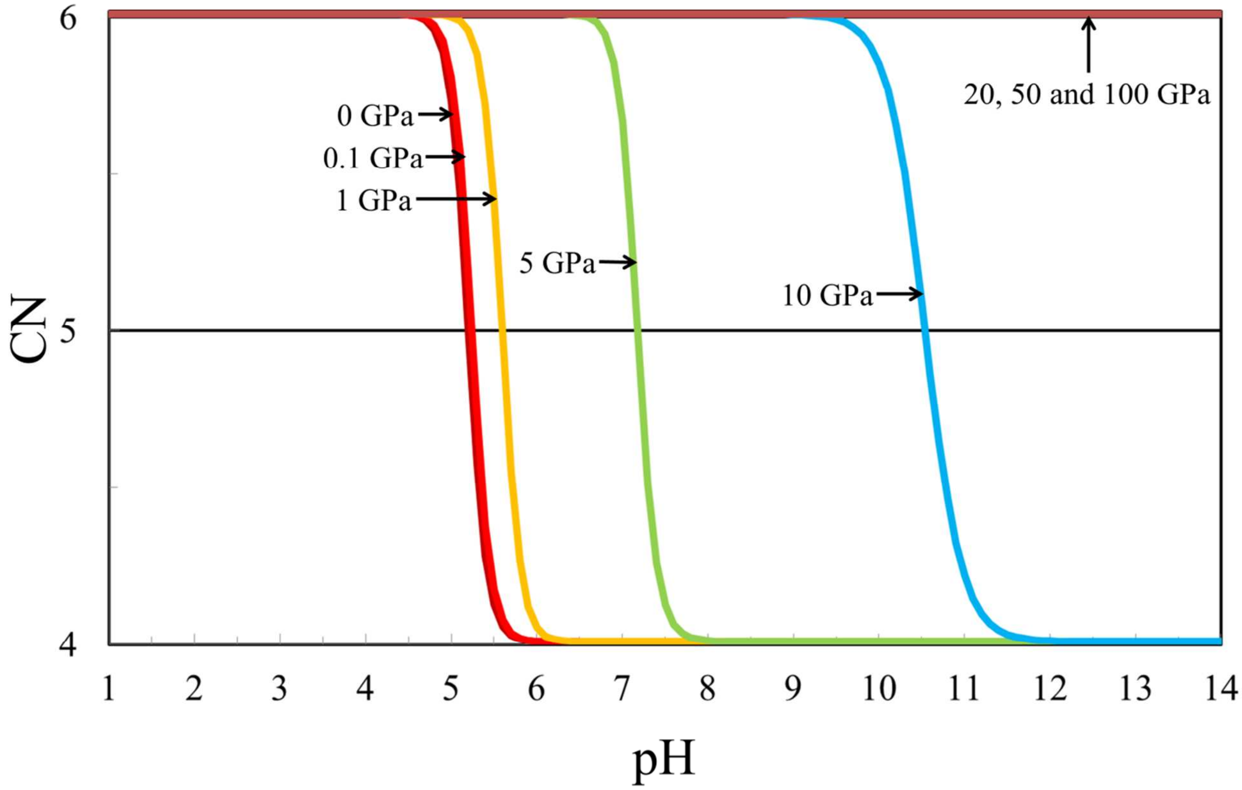

Figure 3: The average total coordination number (CN) of all species is plotted against solution pH for 8 contours corresponding to external pressures of 0, 0.1, 1, 5, 10, 20, 50 and 100 GPa. Note that curves are overlying for 0 and 0.1 GPa, those corresponding to 20, 50 and 100GPa are also superimposed.

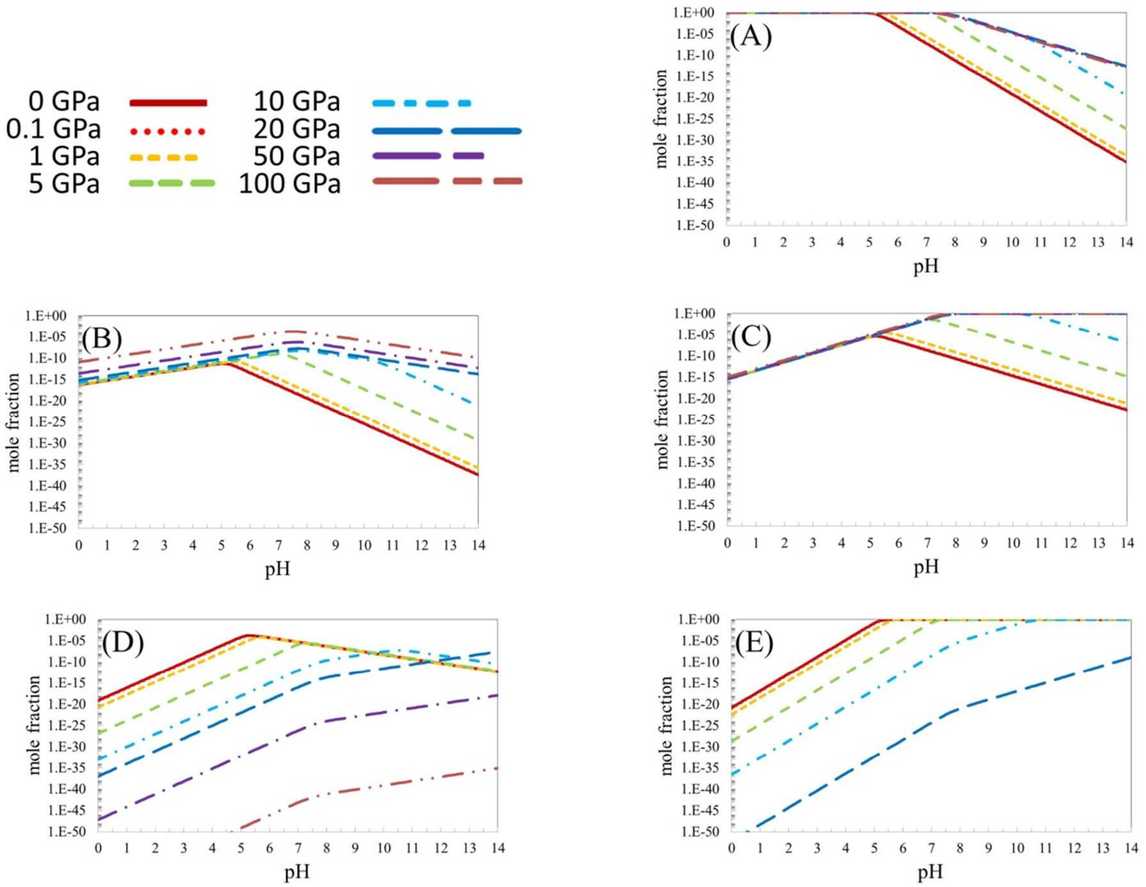

Figure 4: The evolution of the mole fraction distributions of the aqua species (Figure 4A) and the 1st (Figure 4B), 2nd (Figure 4C), 3rd (Figure 4D) and 4th (Figure 4E) hydrolysis products as a function of pH for 8 contours corresponding to external pressures of 0, 0.1, 1, 5, 10, 20, 50 and 100 GPa.